Cancer Chemother Pharmacol (2009) 64:793–802
DOI 10.1007/s00280-009-0929-5

ORIGINAL ARTICLE

Pro-apoptotic and cytostatic activity of naturally occurring cardenolides

Elena Bloise · Alessandra Braca · Nunziatina De Tommasi · Maria Antonietta Belisario

Received: 3 November 2008 / Accepted: 5 January 2009 / Published online: 28 January 2009

Abstract
Purpose Cardenolidde are steroid glycosides which are known to exert cardiotonic effects by inhibiting the Na^+/K^+-ATPase. Several of these compounds have been shown also to possess anti-tumor potential. The aim of the present work was the characterization of the tumor cell growth inhibition activity of four cardenolides, isolated from *Periploca graeca* L., and the mechanisms underlying such an effect.
Methods The pro-apoptotic and cytostatic effect of the compounds was tested in U937 (monocytic leukemia) and PC3 (prostate adenocarcinoma). Characterization of apoptosis and cell cycle impairment was obtained by cytofluorimetry and WB.
Results Periplocymarin and periplocin were the most active compounds, periplocymarin being more effective than the reference compound ouabain. The reduction of cell number by these two cardenolides was due in PC3 cells mainly to the activation of caspase-dependent apoptotic pathways, while in U937 cells to the induction of cell cycle impairment without extensive cell death. Interestingly, periplocymarin, at cytostatic but non-cytotoxic doses, was shown to sensitize U937 cells to TRAIL.
Conclusions Taken together, our data outline that cardiac glycosides are promising anticancer drugs and contribute to the identification of new natural cardiac glycosides to obtain chemically modified non-cardioactive/low toxic derivatives with enhanced anticancer potency.

Keywords Cardenolides · PC3 · U937 · Apoptosis · Cell cycle · TRAIL

E. Bloise · N. De Tommasi · M. A. Belisario (✉)
Dipartimento di Scienze Farmaceutiche,
Università di Salerno, Via Ponte Don Melillo,
84084 Fisciano, SA, Italy
e-mail: mabelisario@unisa.it

A. Braca
Dipartimento di Chimica Bioorganica e Biofarmacia,
Università di Pisa, Via Bonanno 33, 56126 Pisa, Italy

Introduction

The class of steroid-like compounds designed cardiac glycosides includes well-known drugs such as digoxin, digitoxin, and ouabain. These compounds have been used for many years mainly for the treatment of cardiac congestion and some types of cardiac arrhythmias [1]. The known and accepted mode of action of cardiac glycosides is inhibition of ubiquitous plasma membrane Na^+/K^+-ATPase [2]. Recent findings suggest for Na^+/K^+-ATPase a new interesting role as signal transducer, demonstrating its involvement not only in maintaining electrolyte balance but also in several biological processes [3, 4]. Over the years there have been various reports suggesting that cardiac glycosides may have an anticancer utilization [5]. Evidences of the antineoplastic potential of cardiac glycosides have been obtained in in vitro studies. Their ability to induce cell death in cells from tumors of different hystogenetic origin [6–9] and to interfere with cell adhesion and cell–cell interaction processes has been demonstrated [10]. In addition to these studies on cancer cells in vitro, the most relevant evidences of the beneficial effects of cardiac glycosides in cancer treatment were drawn from epidemiological data. The death rate and cancer recurrence turned out to be lower in women with breast cancer treated with digitalis than in non-treated patients [11]. Moreover, Haux et al. [12] observed a reduced incidence of leukemia/lymphoma and kidney/urinary

tract tumors in subjects with elevated plasmatic concentrations of digitoxin.

One of the main obstacles for the clinical utilization of these molecules as antitumoral are their narrow range of therapeutic safety: in most of cell culture studies, in fact, the doses of compounds used to induce apoptosis are considered cardiotoxic; moreover different species of model animals show a wide variability in susceptibility of these cardiac glycosides making problematic extrapolation from animal model in the human [13]. However, Langenhan et al. [14] showed that sugar modifications by neoglycorandomization, can dramatically, and independently, modulate both cytotoxic properties and the Na^+/K^+-ATPase inhibitory properties of cardiac glycosides. Moreover, Daniel et al. [15] found that the removal of the chemical group responsible for inhibition of Na^+/K^+-ATPase did not abrogate the proapoptotic effect of some cardiac glycosides, thus suggesting that in addition to inhibition of Na^+/K^+-ATPase, other mechanisms might be responsible for apoptotic induction by these compounds. Several mechanisms have been proposed to underlie the antineoplastic potential of cardiac glycosides [16], which include inhibition of glycolisis, increase of intracellular Ca^{++} and hydrogen peroxide, cellular acidification, inhibition of topoisomerase II, regulation of fibroblast growth factor-2, inactivation of transcription factor NF-kB.

In our previous work [17] we investigated the antiproliferative activity of cardenolides isolated from *Periploca graeca* L. (Asclepiadaceae) small branches, a perennial liana occurring wild in southeast European and west Asian countries, and we found that 17β-configuration of the lactone ring is crucial for the cytotoxic effect, together with the presence of a sugar residue at C-3, while no significant changes in the IC_{50} values were observed between the mono-, di-, and tri-glycosilated compounds. In the present study, we tested the antiproliferative activity of the most abundant compounds periplogenin, periplocymarin, periplocin, and 17α-periplocin (Chart 1) in U937 (human monocytic leukemia) and PC3 (androgen-independent prostate adenocarcinoma) cell lines. The mechanism(s) underlying the growth inhibition activity of the more active compounds periplocymarin and periplocin were investigated. Moreover, the capability of periplocymarin to sensitize U937 cells to TRAIL-induced apoptosis was studied.

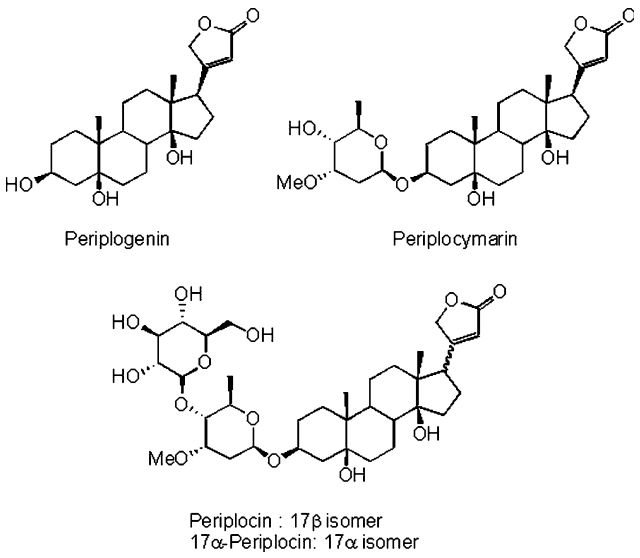

Chart 1

Materials and methods

Chemicals

Fetal bovine serum (FBS) was from Bio-Whittaker, CellTiter-Blue® Reagent was from Promega. Antibodies*:* anti-caspase-3 (rabbit polyclonal, AAP113) was obtained from Stressgen (CA, USA), anti-α tubulin (mouse monoclonal, B-5-1-2) from Sigma-Aldrich (MO, USA), peroxidase-conjugated secondary antibodies goat anti-rabbit (111-035-003) and goat anti-mouse IgG (115-035-003) from Jackson ImmunoResearch (PA, USA). Porcine cerebral cortex Na^+/K^+-ATPase, ouabain, and all the other chemicals were purchased from Sigma-Aldrich (MO, USA). Human recombinant *Superkiller* TRAIL (tumor necrosis factor-related apoptosis inducing ligand, ALX-201-115), monoclonal antibody to human TRAIL receptor DR5 (ALX-804-298) and isotype control immunoglobulins (mouse IgG1, ALX-804-870) were purchased from Alexis Biochemicals. FITC-conjugated secondary antibody goat anti-mouse IgG (115-095-003) was from Jackson ImmunoResearch (PA, USA).

Periplogenin, periplocymarin, periplocin, and its 17α-isomer were isolated from *P. graeca* L. small branches. The dried powdered stems (480 g) were extracted with *n*-hexane, $CHCl_3$, $CHCl_3$-MeOH (9:1), and MeOH, to give 3.2, 6.7, 8.6, and 16.0 g of the respective residues. The $CHCl_3$ extract (6.0 g) was purified by flash silica gel column (6.0 × 16.0 cm), eluting with $CHCl_3$ followed by increasing concentrations of MeOH (between 1 and 100%) in $CHCl_3$. Fractions of 30 mL were collected and grouped into ten fractions (1–10). Fractions 2 (330 mg) and 6 (400 mg) were subjected to RP-HPLC on a C_{18} μ-Bondapak column (30 cm × 7.8 mm, flow rate 2.0 mL min^{-1}) with MeOH-H_2O (3:2) to afford pure periplogenin and periplocymarin from fraction 2 and 17α-periplogenin and periplocin from fraction 6, respectively. The structural characterization of pure compounds was obtained by NMR and MS analyses.

Cells and treatment

Human monocytic leukemia U937 and androgen independent prostate cancer PC3 cells were from Cell Bank in

GMP-IST (Genova, Italy). Cells were maintained in RPMI 1640 medium supplemented with 10% (v/v) FBS, 2 mM L-glutamine and antibiotics (100 U/mL penicillin, 100 μg/mL streptomycin) at 37°C in humidified atmosphere with 5% CO_2. To ensure logarithmic growth, cells were subcultured every 2 days. Human peripheral blood mononuclear cells (PBMC) were isolated from buffy coats of healthy donors (kindly provided by the Blood Center of the Hospital of Battipaglia, Salerno, Italy) by using standard Ficoll–Hypaque gradients. Freshly isolated PBMC contained 95.6 ± 2.7% live cells. Tested compounds and ouabain, used as a reference molecule, were dissolved in DMSO and stored as stock solutions (4 mM) at −20°C. Working solutions, prepared in PBS, were used to obtain the desidered concentrations in culture medium. In all experiments, the final concentration of DMSO did not exceed 0.013% (v/v).

Na^+/K^+-ATPase inhibition assay

The Na^+/K^+-ATPase inhibitory potency of tested molecules was evaluated in a cell-free system. Na^+/K^+-ATPase activity was monitored spectrophotometrically by the molybdate assay according to Jortani et al. [18] Samples containing the buffer alone were used as no-inhibitor control and results were expressed as percentage of ATPase activity with control considered as 100%.

Cell proliferation and viability

U937 and PC3 in 96 well-plates (2×10^4/well and 1×10^4/well, respectively) were exposed to increasing concentrations of cardenolides or vehicle only for the indicated times. Then, the number of cells was quantified by using the CellTiter-Blue® Cell Viability assay. The CellTiter-Blue® Reagent was added and the cultures incubated for 1 h before fluorescence (λexc 560 nm, λem 590 nm) readings were taken. At these wavelengths, none of tested compounds have a fluorescence signal.

Flow cytometry analyses

Apoptosis detection

The DNA content was evaluated by propidium iodide (PI) incorporation in permeabilized cells according to the available protocol [19] and flow cytometry. Data from 10,000 events per sample were collected and the percentage of the elements in the hypodiploid region was calculated using the CellQuest software. PI staining of non-permeabilized cells was taken as a measure of necrosis. The percentage of cells actively undergoing apoptosis was also evaluated by Annexin V/PI test according to the manufacturer's instructions (Human Annexin-V/FITC kit, Bender Medsystem, CA, USA). Annexin V binds phosphatidylserine residues exposed during apoptosis and PI stains the cellular DNA of those that have compromised cell membranes. Green (Annexin V-FITC) and red (PI) fluorescence of individual cells were measured by flow cytometry. Electronic compensation was required to exclude overlapping of the two emission spectra.

Depolarization of mitochondria

Loss of mitochondrial transmembrane potential was determined using the potential sensitive probe tetramethylrhodamine ethyl ester (TMRE) [20]. Briefly, control and treated PC3 cells were loaded at 37°C with TMRE dye (5 nM, final concentration). After 30 min, cells were harvested and fluorescence intensity was evaluated by flow cytometry (FL2 channel).

Cell cycle analysis

To evaluate cell cycle distribution, control and treated U937 cells were harvested and nuclei were labeled with PI as described for apoptosis detection and analyzed by flow cytometry. Data from 20,000 events per sample were collected and the relative percentage of the cells in G_0/G_1, S and G_2/M phases of the cell cycle were determined using the MODFIT software (Becton Dickinson, San Jose, CA, USA).

Western blot

Activation of the effector caspase-3 was evaluated by measuring the extent of the 32-kDa proenzyme (CPP32) processing to generate 17- and 12-kDa fragments. Western blot analyses were performed as previously described [21]. Signals were visualized using the enhanced chemiluminescence Western blotting detection system according the manufacturer's instructions (Amersham, USA).

Immunofluorescence

U937 cells (2×10^5) were washed twice with PBS and incubated with saturating amounts of mouse anti-TRAIL-R5, or an appropriate isotype control antibody for at least 1 h on ice. After being washed once, the cells were exposed to a FITC-conjugated goat anti-mouse for an additional hour. Then cells were rinsed twice in PBS, resuspended in the same buffer, and analyzed by flow cytometry. Excitation wavelength used for FITC was 488 nm; the emitted green fluorescence (λ_{max} 520 nm) was detected using FL-1 band-pass filter. A total of 20,000 cells were analyzed for each sample. Data analysis was performed by using the Cell Quest software.

RT-PCR

U937 cells were seeded in 12-well plates (5×10^5 cells/well) and exposed for 24 h to 100 nM periplocymarin or vehicle only. To detect the expression of DR5 and housekeeping gene β-actin, total cellular RNA was extracted from 5×10^5 cells using TRIzol ®LS Reagent (Invitrogen, Carlsbard, CA, USA) according to the manufacturer's instructions. cDNAs were synthesized from 2 μg of total RNA using the SuperScript First-Strand Synthesis System kit for RT-PCR (Invitrogen, Carlsbard, CA, USA) with the supplied oligo(dT) primers under conditions described by the manufacturer. The simultaneous amplification of DR5 and β-actin was performed in a 20 μL reaction mixture using cDNA derived from 200 ng of RNA (10% of first-strand reaction mix) using Platinum® *Taq* DNA Polymerase (Invitrogen, Carlsbard, CA, USA). The following specific primer pairs were used in polymerase chain reaction: DR5 sense, 5′-GCTTCATGGACAATGAGATAAAGGTGGCT-3′; DR5 antisense, 5′-CCAAATCTCAAAGTACGCACAAACGG-3′; β-actin sense, 5′-TGACGGGGTCACCCACACTGTGCCCATCTA-3′; β-actin antisense, 5′-CTAGAAGCATTTGCGGTGGACGATGGAGGG-3′, giving products of 502 and 661 base paires respectively. PCR products were size-fractionated by 1,5% agarose gel electrophoresis and the resulting bands were detected by ethidium bromide staining. Images were acquired with a Gel Doc System (Gel Doc 2000, BioRad).

Statistical analysis

Data are expressed as the mean ± standard error of the mean (SEM) of at least three independent experiments, performed in duplicate, showing similar results. Differences between treatment groups were analyzed by the student *t* test or by ANOVA test. Differences were considered significant when $P < 0.05$.

Results

Antiproliferative activity

Exponentially growing cultures of U937 and PC3 cells were incubated with increasing doses of each cardenolide and the number of viable cells was evaluated after 24 h. The EC_{50} value (half maximal effective concentration) for each compound was calculated from the respective dose–response curves (Table 1). In both cell lines cardenolides displayed the same EC_{50} ascending order, even though U937 proved more susceptible than PC3. Periplocymarin and periplocin were active in a nanomolar range of doses like the reference compound ouabain [6], while periplogenin and 17α-periplocin displayed their inhibitory activity at doses higher than 1 and 2.5 μM, respectively. Changes in the cell number by periplocymarin and periplocin were also monitored as a function of incubation time without any further loading of the drugs (Fig. 1). As indicated by the slopes of the growth curves, cardenolide-treated PC3 cells seemed to recover with the time a proliferation rate comparable to that of controls; by contrast, U937 showed a more marked delay in recovering the proliferation rate of controls, thus suggesting that periplocymarin and periplocin might cause the reduction of the cell number through different mechanisms.

Table 1 Cancer cell growth inhibition by cardenolides

Compound	EC_{50} (nM)[a]	
	PC3	U937
Periplogenin	1410 ± 65	1200 ± 56
Periplocymarin	180 ± 10	83 ± 9
Periplocin	267 ± 21	120 ± 10
17α-periplocin	>2500	>2500
Ouabain	210 ± 18	94 ± 11

PC3 and U937 cells were cultured in the absence and in the presence of increasing doses of cardenolides or ouabain for 24 h and the number of cells was determined as described in "Materials and methods". Data represent the mean values ± SEM of three experiments performed in quintuplicate

[a] Cell growth inhibition potency is expressed as EC_{50}, which is the effective concentration of the compound that causes a 50% reduction in cell number relative to untreated cells. EC_{50} values for each isomer were calculated from the dose-response curves

Inhibition of Na^+/K^+-ATPase

Next, we evaluated the inhibitory activity of cardenolides against porcine Na^+/K^+-ATPase in a cell-free system. Figure 2 shows that periplocymarin and periplocin, the most active as growth inhibitor, displayed also the highest Na^+/K^+-ATPase inhibitory activity. Interestingly, irrespective of whether periplocymarin growth inhibition potency was comparable to that of ouabain, its Na^+/K^+-ATPase inhibition activity was, even slightly, lower than that of the reference compound [18].

Pro-apoptotic activity of cardenolides

A reduction of tumor cell number might depend upon the occurrence of cell death (cytotoxic effect) or cell cycle block (cytostatic effect). Thus, to characterize the mechanisms underlying the antiproliferative effects of periplocymarin and periplocin on PC3 and U937, the ability of the two cardenolides to induce cell death (by apoptosis or necrosis) or to affect cell cycle progression was further

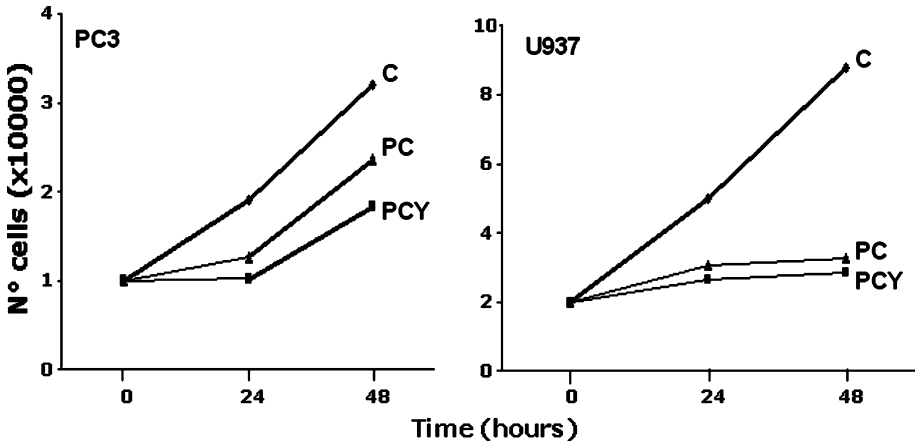

Fig. 1 Kinetics of PC3 and U937 growth inhibition by cardenolides. Cells were cultured in presence of a fixed dose (*PC3*, 200 nM; U937, 100 nM) of periplocymarin (*PCY*) and periplocin (*PC*) up to 48 h. Control cells (*C*) received only the vehicle. The number of cells was quantified as described in "Materials and methods". Data represent the mean values ± SEM of three experiments performed in quintuplicate

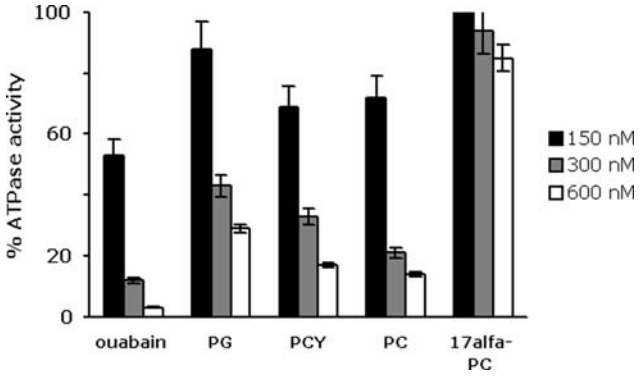

Fig. 2 ATPase inhibition by cardenolides. Inhibition of porcine Na^+/K^+ ATPase activity by periplogenin (*PG*), periplocymarin (*PCY*), periplocin (*PC*), 17α-periplocin (*17α-PC*) and by the reference compound ouabain was evaluated as described in "Materials and methods". Data are expressed as percentage of sodium pump activity. Results represent the mean values ± SEM of three separate experiments performed in duplicate

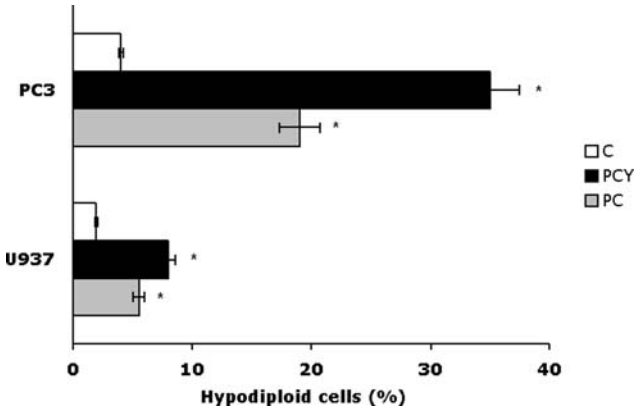

Fig. 3 Cardenolides induced apoptosis in cancer cells. PC3 and U937 cells were exposed for 24 h to 200 or 100 nM of periplocymarin (*PCY*) and periplocin (*PC*), respectively. Control cells were exposed to vehicle only (*C*). DNA fragmentation was evaluated by flow cytometry (PI staining of permeabilized cells) and results are expressed as the percentage of the total cell population analyzed (10,000 events). Data reported are the mean values ± SEM from three separate experiments. $^*P < 0.05$

investigated. PC3 and U937 cells were exposed for 24 h to doses of periplocymarin and periplocin close to the respective EC_{50} values in the two cell lines. The induction of DNA fragmentation (hypodiploid cells), assessed by flow cytometry after cell permeabilization and PI staining, was taken as an evidence of apoptotic mode of cell death. As summarized in Fig. 3, both compounds displayed significant pro-apoptotic activity in PC3 cells. In particular, the percentages of apoptotic cells exposed to periplocymarin and periplocin were about nine and fivefold higher than that of control cells, respectively. In contrast, in U937 cells both the two cardenolides turned out to cause only a slight increase in the percentage of apoptotic cells. Very high doses (>1,000 nM) of periplocymarin and periplocin were required to observe a 30–40% of apoptotic cells.

It must be pointed out that doses ≤300 nM of periplocymarin or periplocin did not cause PC3 and U937 necrotic death as assessed by Tripan blue exclusion assays or PI staining of non-permeabilized cells (data not shown).

Analysis of cardenolide-induced apoptosis in PC3 cells

To get further evidence for periplocymarin-induced apoptotic mode of cell death in PC3 cells, the exposure of phosphatidylserine residues, a hallmark of early apoptosis [22], was evaluated in cells exposed to different doses of the cardenolide for 14 h. Double-staining of cells with Annexin V and PI allows for the discrimination of live cells (unstained with either fluorochrome, Annexin V^-/PI^-) from early apoptotic cells (Annexin V^+/PI^-), late apoptotic cells (Annexin V^+/PI^+) or necrotic cells (stained only with PI). Figure 4, upper panel, shows that periplocymarin caused a dose-dependent increase in the percentage of cells in both early and late apoptosis, without any significant increase in the percentages of necrotic cells (Annexin V^-/PI^+). Figure 4 shows also that the presence of Z-VAD fmk, a pan-caspase inhibitor, strongly reduced, if not completely ablated, the percentage of periplocymarin-induced

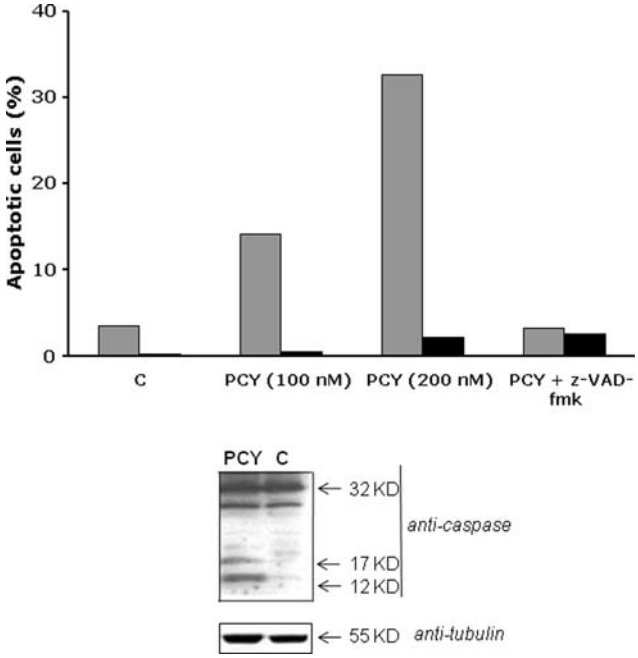

Fig. 4 Periplocymarin induced caspase-dependent apoptosis in prostate cancer cells. *Upper panel* PC3 cells were incubated for 14 h with periplocymarin (PCY) or vehicle only (C). An aliquot of cells was pre-exposed for 1 h to 30 μM z-VAD-fmk before addition of 200 nM PCY. Cells were double-stained with Annexin V-FITC and PI before flow cytometric analysis. *Gray bars* percentages of apoptotic cells (AnnexinV^+/PI^- plus AnnexinV^+/PI^+ cells); *black bars* percentages of necrotic cells (AnnexinV^-/PI^+ cells). *Lower panel* PC3 cells were treated with 200 nM of periplocymarin (*PCY*) or vehicle (*C*) for 14 h. Activation of pro-caspase 3 was evaluated by Western blot as described in "Materials and methods". The amount of proteins loaded was equal in all lanes of the gel, as verified on parallel immunoblots probed with anti-tubulin antibody

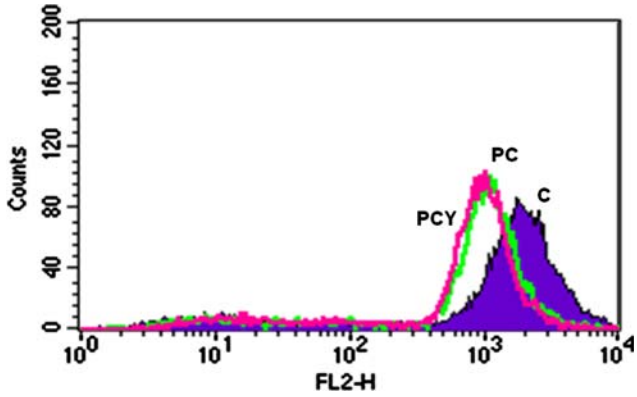

Fig. 5 Alteration of the mitochondrial transmembrane potential in prostate cancer cells. Mitochondrial depolarization was assessed by flow cytometry in PC3 cells treated for 14 h with 200 nM of periplocymarin (*PCY*), periplocin (*PC*) or vehicle only (*C*, *solid filled gray histograms*) and then loaded with TMRE. The histograms are representative of three experiments performed in duplicate with similar results

phosphatidylserine exposure. This result suggested the involvement of caspases in the apoptotic death response elicited by periplocymarin. Accordingly, the activation of the effector caspase-3 was found in periplocymarin-treated PC3 cells. The blots reported in Fig. 4, lower panel, show the presence of the 17 and 12-kDa digestion fragments in cardenolide-exposed cells, while only the zymogen (32 kDa) was detectable in controls.

Mitochondria have been shown to play a central role in apoptosis signaling pathways, especially the intrinsic signaling pathway [23]. Mitochondria initiating the apoptotic cascade have altered mitochondrial transmembrane potential ($\Delta\Psi m$) and permeabilized outer membrane, resulting in the release of soluble pro-apoptotic proteins. Thus, changes of $\Delta\Psi m$ in periplocymarin- and periplocin-treated PC3 were monitored to assess the involvement of mitochondria in cardenolide-induced apoptosis. As shown in Fig. 5, cell treatment with both compounds caused a significant increase in the percentage of cells with depolarized mitochondria, as compared to control cells.

Cell cycle impairment by cardenolides

The finding that periplocymarin and periplocin, at concentrations effective in reducing the U937 cell number by 50%, exhibited very low pro-apoptotic activity in this cell line, prompted us to investigate the effects of the two cardenolides on U937 cell cycle progression. Cells were exposed for 24 h to 100 nM of each cardenolide and cell cycle distribution was evaluated in PI labeled nuclei (as for apoptosis detection) by flow cytometry. According to our hypothesis, periplocymarin and periplocin impaired U937 cell cycle progression, by causing cells to accumulate in G_2/M (Fig. 6). Conversely, PC3 cells exposed to 200 nM ($\cong EC_{50}$) of periplocymarin or periplocin for 24 h displayed only a slight increase in the percentage of cells in G_0/G_1, but substantially the cell cycle profile was similar to that of control cells (data not shown).

Periplocymarin sensitizes U937 toward TRAIL-induced apoptosis

First we evaluated the amount of TRAIL, a cytokine of the TNF family with selective antitumor activity [24], required to induce apoptosis in U937. Cells were exposed for 24 h to increasing doses of TRAIL and the percentage of hypodiploid cells was measured by flow cytometry after PI labeling of permeabilized cells. Up to 70 ng/ml of the drug, the percentage of apoptotic cells was only slight increased (<10%) as compared to control (3%). At 150 ng/ml TRAIL the percentage of hypodiploid cells raised to 30% (data not shown).

To evaluate the capability of periplocymarin to sensitize U937 to apoptosis induced by TRAIL, cells were exposed for 24 h to sub-optimal doses of both compounds, alone or

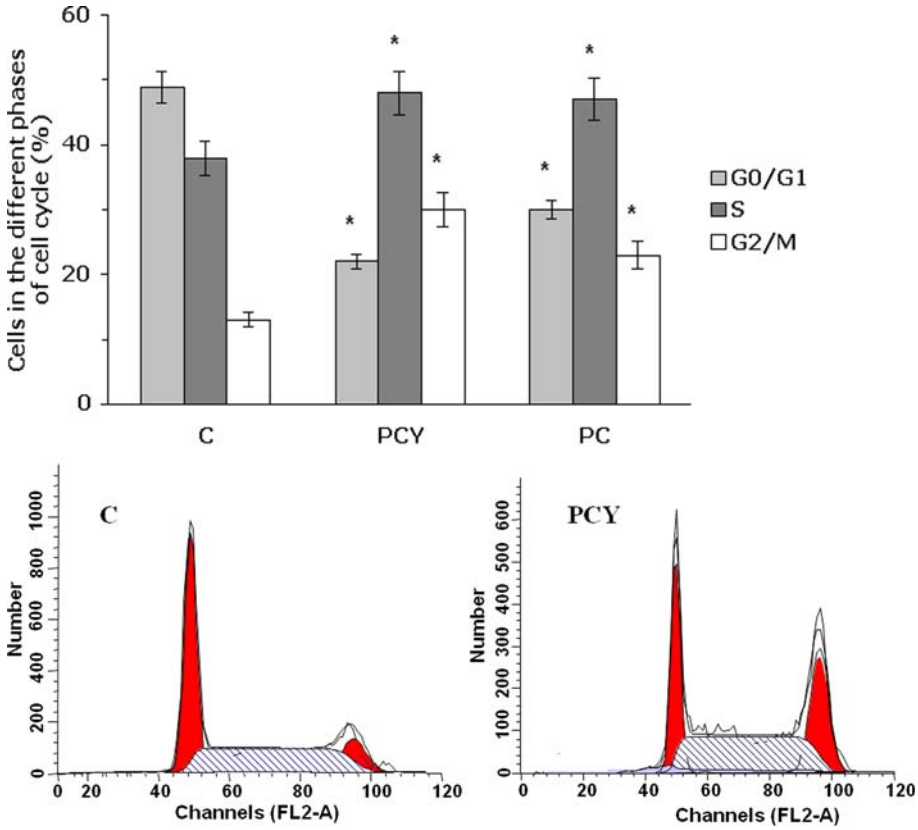

Fig. 6 Effect of cardenolides on cell cycle progression in U937 cells. *Upper panel* U937 cells were incubated for 24 h with 100 nM of periplocymarin (*PCY*), periplocin (*PC*), or the vehicle only (*C*). Cell cycle distribution was evaluated by flow cytometry after PI staining of nuclei. Data are expressed as the percentage of the total cell population in each phase of the cell cycle. Results indicate the mean values ± SEM of three separate experiments. $*P < 0.05$ versus C. *Lower panel* Representative histograms of cell cycle distribution of U937 cells treated with vehicle only or PCY

combined, and the percentages of apoptotic cells were measured. As summarized in Fig. 7 (upper panel), while TRAIL alone (10 ng/ml) induced less than 10% of hypodiploid cells, its combination with periplocymarin caused more than 50% cells to undergo apoptosis. Interestingly, PBMC did not undergo apoptosis either when exposed to the single agents or their combination. The sensitization of neoplastic cells to TRAIL was detectable also at earlier times as assessed by evaluating the exposure of phosphatidylserine residues in U937 cells co-treated with periplocymarin and TRAIL for 16 h (Fig. 7, lower panel).

The next step was to evaluate whether the observed periplocymarin-induced sensitization was due to an increased surface membrane expression of DR5, the only functional receptor in U937 cells [25]. As shown by immunofluorescence profiles reported in Fig. 8, the extent of anti-TRAIL-R5 antibody binding to the receptor was effectively enhanced in cardenolide-treated U937 as compared to control cells. Moreover, by means of RT-PCR analysis, we demonstrated that periplocymarin induced an increase in DR5 receptor mRNA levels (Fig. 9).

Discussion

In the present study, we evaluated the cell growth inhibition activity of periplogenin, periplocymarin, periplocin, and its 17α-isomer, four naturally occurring cardenolides [17], in two tumor-derived cell lines. PC3, a human prostate cancer cell line, and U937 cells, a human monocytic leukemia cell line, were chosen as an experimental model since the antitumor potential of cardiac glycosides in prostate cancer and leukemia cell lines has been previously demonstrated [6, 26, 27].

Despite the close similarity, tested compounds displayed different cell growth inhibitory potency. Periplocymarin and periplocin were the most effective as cell growth inhibitors, being active in a nanomolar range of doses like the reference compound ouabain [6]. The different ability of tested compounds to interact with porcine Na^+/K^+ ATPase seems to account, at least in part, for their different growth inhibition potency. 17α-periplocin and periplogenin are the less effective as Na^+/K^+-ATPase inhibitors and displayed also the lowest antiproliferative activity. It is well established that the 17β-configuration of the lactone is crucial for the interaction with the pump [28] and that genines are less potent than glycosides [18]. The difference in the time-dependent kinetics of inhibition suggested that periplocymarin and periplocin, the most effective as cell growth inhibitors, activated different response in the two cell lines. Accordingly, we found that the reduction of cell number by the two cardenolides was due to the activation of apoptotic pathways in PC3 cells, while in U937 cells to the induction of cell cycle impairment. One possible explanation for the

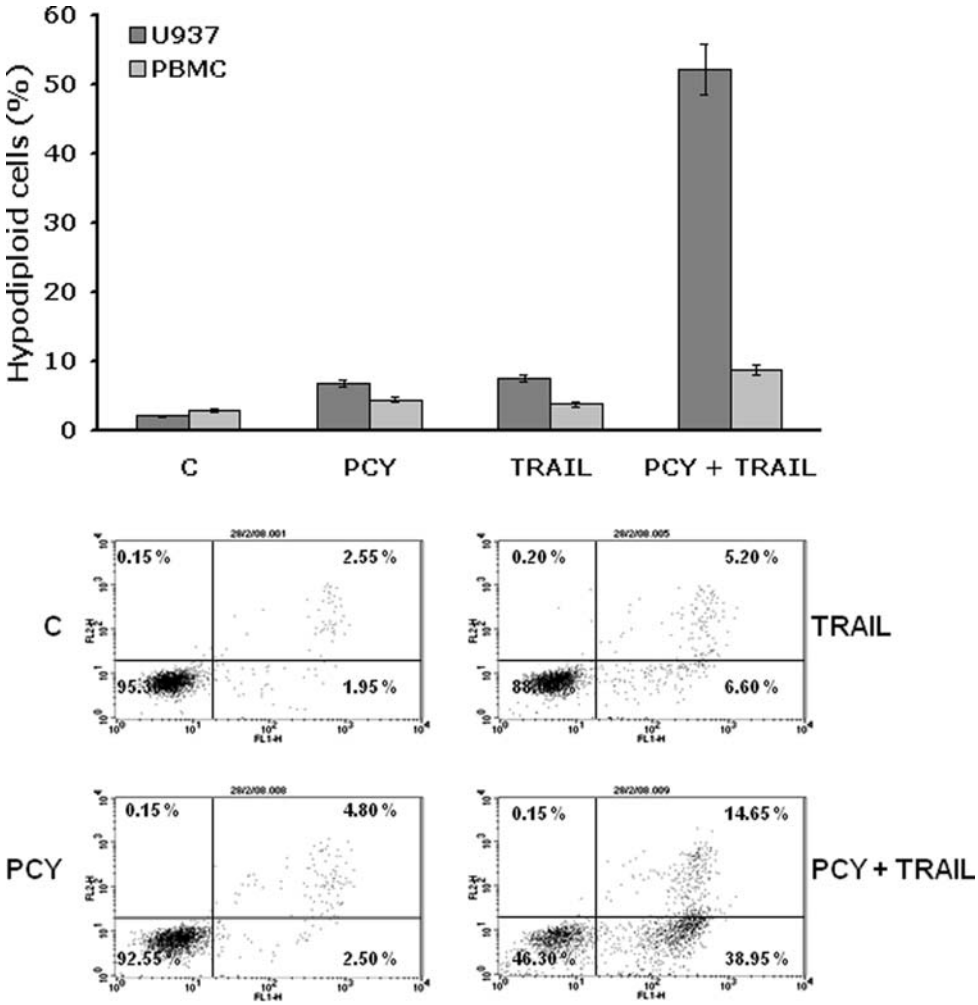

Fig. 7 Periplocymarin sensitized U937 cells but not normal cells to TRAIL. U937 cells and PBMC were treated simultaneously with 100 nM periplocymarin (*PCY*) and 10 ng/ml of TRAIL alone or in combination. Control cells were incubated with vehicle only (*C*). *Upper panel* 24 h following cell treatment, DNA fragmentation was evaluated by flow cytometry and results are expressed as the percentage of the total cell population analyzed (10,000 events). Data reported are the mean values ± SEM from three separate experiments. *Lower panel* 16 h following treatment, U937 cells were double-stained with Annexin V-FITC and PI and analyzed by flow cytometry. The percentage shown represents the percentage of cells in the designated quadrants (*Lower left* viable cells, Annexin$^-$/PI$^-$; *lower right* early apoptotic cells, Annexin$^+$/PI$^-$; *upper right* late apoptotic cells, Annexin$^+$/PI$^+$; *upper left* necrotic cells, Annexin$^-$/PI$^+$). *Dot plots* are representative of two replicate experiments with similar results

different responses elicited by tested cardenolides in PC3 and U937 cells might be that different isoforms of Na^+/K^+-ATPase proteins are expressed in these two cell lines. Na^+/K^+-ATPase is an oligomer composed of three polypeptides, α, β subunits and the auxiliary FXYD subunit, the first containing the "catalytic" site and the binding sites for ATP and glycosides [29]. The main isoforms of α subunits (α1, α2, and α3) have been characterized [30]. Though Na^+/K^+-ATPase signaling has been reported to be primarily associated with α1 isoform, also the other isoforms seem to be relevant as modulator of α1-mediated signaling [30]. PC3 cells were found to express both the α1 and α3, while U937 express only the α1 isoform [31, 32]. Moreover, a different composition of PC3 and U937 plasma membrane might also contribute to the different effects observed in the two cell lines. Data reported by Raghavendra et al. [33] supported the latter hypothesis. They found that oleandrin, a naturally occurring cardiac glycoside, induced apoptosis in human cancer cells, but not murine, and attributed such a difference to a different plasma membrane composition in the two species.

The apoptotic mode of cell death induced by periplocymarin in PC3 cells was confirmed by the occurrence of phosphatidylserine externalization, a hallmark of early apoptosis, and by mitochondrial potential disruption. The apoptotic process activated by periplocymarin involved a caspase-dependent pathway, as demonstrated by the activation of caspase 3 and the reversion of apoptotic cell death in the presence of the pan-caspase inhibitor, Z-VAD fmk. The pro-apoptotic potential displayed by periplocymarin in androgen-independent prostate cancer cells was comparable to that of ouabain [6], as both compounds are effective at nanomolar concentrations.

In U937 cells, periplocymarin caused cells to arrest in the G_2/M phase of cell cycle but had very low effect on cell viability. Kometiani et al. [34] showed that ouabain treatment of MDA-MB-435s breast cancer cell line had no effect on cell viability but resulted in the arrest of proliferation. They observed that ouabain caused an increase in the levels of cell cycle inhibitor $p21^{Cip1}$ and subsequent growth arrest. According to previous findings [15, 16], we found that periplocymarin exhibited low cytotoxic effects on

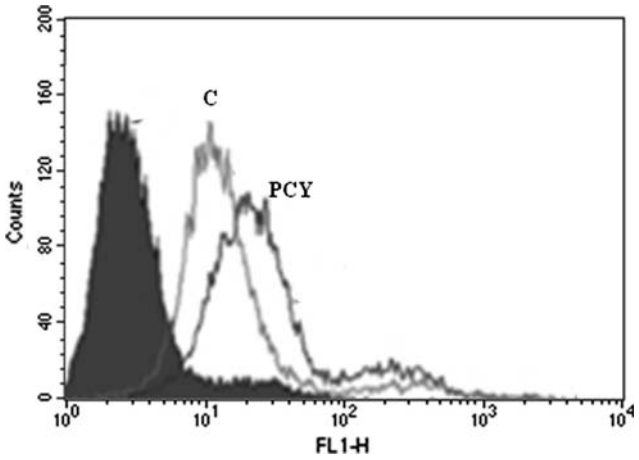

Fig. 8 Effect of periplocymarin on TRAIL receptor expression. Cell surface expression of TRAIL receptor was determined by cytometric analysis as described in "Materials and methods". The histograms, representative of three independent experiments, show the level of receptor-based fluorescence in control cells (*C*) and in periplocymarin-treated U937 (*PCY*) exposed to the drug for 18 h (*open histograms*) in relation to isotype control (*solid filled histograms*). TRAIL receptor expression on cell surface correlates with FITC fluorescence intensity monitored on FL1 channel

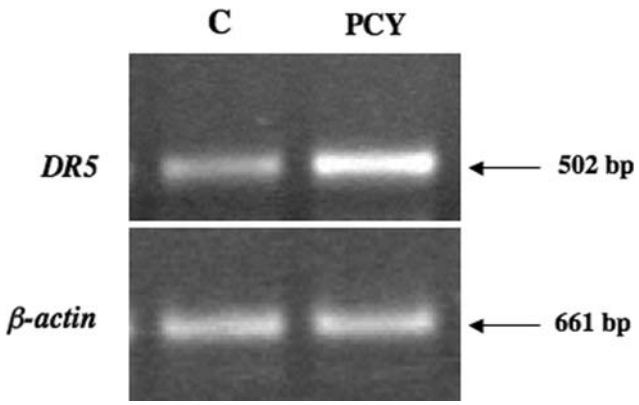

Fig. 9 DR5 TRAIL receptor mRNA expression. U937 cells were exposed to 100 nM periplocymarin (*PCY*) or vehicle only for 10 h and the expression of DR5 mRNA was evaluated by RT-PCR. Expression of β-actin was used as control of RNA integrity and equal gel loading. *Arrows* indicate the size of fragments

human peripheral blood mononuclear cells (PBMC), as the number of cells undergoing apoptotic death after cardenolide-treatment was less than doubled as compared to untreated ones.

The tumor necrosis factor (TNF)–related apoptosis-inducing ligand (TRAIL) is a potential new anticancer drug because it selectively induces apoptosis in a variety of tumor cells, but it is relatively non-toxic to normal cells [35]. Unfortunately, cancer cells are often resistant to TRAIL-induced apoptosis [36, 37]. Oleandrin and other cardiac glycosides were shown to sensitize lung cancer cells to TRAIL-induced apoptosis by up-regulation of death receptors 4 (DR4) and 5 (DR5) on both RNA and protein levels [38]. U937 leukemia-derived cells were shown to be able to escape cell death triggered by low doses of TRAIL [39]. Here we demonstrated that periplocymarin, at doses causing an arrest in G_2/M without extensive cell death, sensitized U937 cells to non-apoptotic doses of TRAIL. The effect seems to be due to the cardenolide-induced enhancing of surface membrane expression of DR5, the TRAIL receptor expressed in U937 cells [25]. However, Inoue et al. [40] found that the increase of TRAIL receptors induced by histone deacetylase (HDAC) inhibitors was not sufficient to explain their capability to sensitize lymphoid cells to TRAIL. Thus, the possibility that cardenolides sensitize U937 to TRAIL also by enhancing receptor clustering (due to changes of membrane fluidity and/or ceramide release [41]) or cooperating with the receptor downstream signaling [39] should be considered.

In this work we confirmed the antiproliferative activity of 17β-cardenolides isolated from *P. graeca* L. and we evidenced the capability of periplocymarin to strongly sensitize U937 cells to non-apoptotic dose of TRAIL. Taken together, our data outline that cardiac glycosides are promising anticancer drugs and contribute to the identification of new natural cardiac glycosides. The future goal could be to consider cardiac glycosides as "lead compounds" and to obtain chemically modified non-cardioactive derivatives with enhanced anticancer potency.

Acknowledgments The student Paola Torre contributed to some experiments and results will be included in her degree thesis. This work was supported in part by research grant from the University of Salerno.

References

1. Hauptmann PJ, Garg R, Kelly RA (1999) Cardiac glycosides in the next millennium. Prog Cardiovasc Dis 41:247–254
2. Rahimtoola SH, Tak T (1996) The use of digitalis in heart failure. Curr Probl Cardiol 21:781–853
3. Xie Z, Cai T (2003) Na^+/K^+-ATPase-mediated signal transduction: from protein interaction to cellular function. Mol Interv 3:157–168
4. Aperia A (2007) New roles for an old enzyme: Na^+/K^+-ATPase emerges as an interesting drug target. J Intern Med 261:44–52
5. Newman RA, Yang P, Pawlus AD, Block KI (2008) Cardiac glycosides as novel cancer therapeutic agents. Mol Interv 8:36–49
6. Huang YT, Chueh SC, Teng CM, Guh JH (2004) Investigation of ouabain-induced anticancer effect in human androgen-independent prostate cancer PC-3 cells. Biochem Pharmacol 67:727–733
7. Bielawski K, Winnicka K, Bielawska A (2006) Inhibition of DNA topoisomerases I and II, and growth inhibition of breast cancer MCF-7 cells by ouabain, digoxin and proscillaridin A. Biol Pharm Bull 29:1493–1497
8. Ramirez-Ortega M, Maldonado-Lagunas V, Melendez-Zajgla J, Carrillo-Hernandez JF, Pastelín-Hernandez G, Picazo-Picazo O, Ceballos-Reyes G (2006) Proliferation and apoptosis of HeLa cells induced by in vitro stimulation with digitalis. Eur J Pharmacol 534:71–76

9. Kulikov A, Eva A, Kirch U, Boldyrev A, Scheiner-Bobis G (2007) Ouabain activates signaling pathways associated with cell death in human neuroblastoma. Biochim Biophys Acta 1768:1691–1702
10. Larre I, Ponce A, Fiorentino R, Shoshani L, Contreras RG, Cereijido M (2006) Contacts and cooperation between cells depend on the hormone ouabain. Proc Natl Acad Sci USA 103:10911–10916
11. Stenkvist B, Pengtsson E, Dahlqvist B, Eriksson O, Jarkrans T, Nordin B (1982) Cardiac glycosides and breast cancer, revisited. N Engl J Med 306:484
12. Haux J, Klepp O, Spigset O, Tretli S (2001) Digitoxin medication and cancer; case control and internal dose-response studies. BMC Cancer 1:11
13. Repke KHR, Benga GH, Tager JM (1988) Biomembranes, basic and medical research. Springer, Berlin, pp 161–173
14. Langenhan JM, Peters NR, Guzei IA, Hoffmann FM, Thorson JS (2005) Enhancing the anticancer properties of cardiac glycosides by neoglycorandomization. Proc Natl Acad Sci USA 102:12305–12310
15. Daniel D, Süsal C, Kopp B, Opelz G, Terness P (2003) Apoptosis-mediated selective killing of malignant cells by cardiac steroids: maintenance of cytotoxicity and loss of cardiac activity of chemically modified derivatives. Int Immunopharmacol 3:1791–1801
16. López-Lázaro M (2007) Digitoxin as an anticancer agent with selectivity for cancer cells: possible mechanisms involved. Expert Opin Ther Targets 11:1043–1053
17. Spera D, Siciliano T, De Tommasi N, Braca A, Vessières A (2007) Antiproliferative cardenolides from *Periploca graeca*. Planta Med 73:384–387
18. Jortani SA, Helm RA, Valdes R Jr (1996) Inhibition of Na^+/K^+-ATPase by oleandrin and oleandrigenin, and their detection by digoxin immunoassays. Clin Chem 42:1654–1658
19. Nicoletti I, Migliorati G, Pagliacci MC, Grignani F, Riccardi C (1991) A rapid and simple method for measuring thymocyte apoptosis by propidium iodide staining and flow cytometry. J Immunol Methods 139:271–279
20. Scaduto RC Jr, Grotyohann LW (1999) Measurement of mitochondrial membrane potential using fluorescent rhodamine derivatives. Biophys J 76:469–477
21. Dal Piaz F, Nigro P, Braca A, De Tommasi N, Belisario MA (2007) 13-Hydroxy-15-oxo-zoapatlin, an *ent*-kaurane diterpene, induces apoptosis in human leukemia cells, affecting thiol-mediated redox regulation. Free Radic Biol Med 43:1409–1422
22. Vermes I, Haanen C, Steffens-Nakken H, Reutelingsperger C (1995) A novel assay for apoptosis. Flow cytometric detection of phosphatidylserine expression on early apoptotic cells using fluorescein labelled Annexin V. J Immunol Methods 184:39–51
23. Gogvadze V, Orrenius S (2006) Mitochondrial regulation of apoptotic cell death. Chem Biol Interact 163:4–14
24. Almasan A, Ashkenazi A (2003) Apo2L/TRAIL: apoptosis signaling, biology, and potential for cancer therapy. Cytokine Growth Factor Rev 14:337–348
25. MacFarlane M, Inoue S, Kohlhaas SL, Majid A, Harper N, Kennedy DB, Dyer MJ, Cohen GM (2005) Chronic lymphocytic leukemic cells exhibit apoptotic signaling via TRAIL-R1. Cell Death Differ 12:773–782
26. Mijatovic T, De Nève N, Gailly P, Mathieu V, Haibe-Kains B, Bontempi G, Lapeira J, Decaestecker C, Facchini V, Kiss R (2008) Nucleolus and c-Myc: potential targets of cardenolide-mediated antitumor activity. Mol Cancer Ther 7(5):1285–1296
27. Ihenetu K, Qazzaz HM, Crespo F, Fernandez-Botran R, Valdes R (2007) Digoxin-like immunoreactive factors induce apoptosis in human acute T-cell lymphoblastic leukemia. J Clin Chem 53:1315–1322
28. Schoner W (2002) Sodium pump and steroid hormone receptor. Na^+/K^+-ATPase. Eur J Biochem 269:2423
29. Kaplan JH (2002) Biochemistry of Na^+/K^+-ATPase. Annu Rev Biochem 71:511–535
30. Wasserstrom JA, Aistrup GL (2005) Digitalis: new actions for an old drug. Am J Physiol Heart Circ Physiol 289:H1781–H1793
31. Gilmore-Hebert M, Schneider JW, Greene AL, Berliner N, Stolle CA, Lomax K, Mercer RW, Benz EJ Jr (1989) Expression of multiple Na+, K+-adenosine triphosphatase isoform genes in human hematopoietic cells. Behavior of the novel A3 isoform during induced maturation of HL60 cells. J Clin Invest 84:347–351
32. Duran MJ, Chosseler M, Pressley T (2004) Regulation of Na, K-pump-mediated transport by prolactin in cultured human prostate epithelial cells. Cell Mol Biol 50:809–814
33. Raghavendra PB, Sreenivasan Y, Manna SK (2007) Oleandrin induces apoptosis in human, but not in murine cells: dephosphorylation of Akt, expression of FasL, and alteration of membrane fluidity. Mol Immunol 44:2292–2302
34. Kometiani P, Liu L, Askari A (2005) Digitalis-induced signaling by Na^+/K^+-ATPase in human breast cancer cells. Mol Pharmacol 67:929–936
35. Hao C, Song JH, Hsi B, Lewis J, Song DK, Petruk KC, Tyrrell DL, Kneteman NM (2004) TRAIL inhibits tumor growth but is non-toxic to human hepatocytes in chimeric mice. Cancer Res 64:8502–8506
36. MacFarlane M, Harper N, Snowden RT, Dyer MJ, Barnett GA, Pringle JH, Cohen GM (2002) Mechanisms of resistance to TRAIL induced apoptosis in primary B cell chronic lymphocytic leukaemia. Oncogene 21:6809–6818
37. Todaro M, Lombardo Y, Francipane MG, Alea MP, Cammareri P, Iovino F, Di Stefano AB, Di Bernardo C, Agrusa A, Condorelli G, Walczak H, Stassi G (2008) Apoptosis resistance in epithelial tumors is mediated by tumor-cell-derived interleukin-4. Cell Death Differ 15:762–772
38. Frese S, Frese-Schaper M, Andres AC, Miescher D, Zumkehr B, Schmid RA (2006) Cardiac glycosides initiate Apo2L/TRAIL-induced apoptosis in non-small cell lung cancer cells by up-regulation of death receptors 4 and 5. Cancer Res 66:5867–5874
39. Rosato RR, Almenara JA, Coe S, Grant S (2007) The multikinase inhibitor sorafenib potentiates TRAIL lethality in human leukemia cells in association with Mcl-1 and cFLIPL down-regulation. Cancer Res 67:9490–9500
40. Inoue S, MacFarlane M, Harper N, Wheat LM, Dyer MJ, Cohen GM (2004) Histone deacetylase inhibitors potentiate TNF-related apoptosis-inducing ligand (TRAIL)-induced apoptosis in lymphoid malignancies. Cell Death Differ 11(Suppl 2):S193–S206
41. Dumitru CA, Carpinteiro A, Trarbach T, Hengge UR, Gulbins E (2007) Doxorubicin enhances TRAIL-induced cell death via ceramide-enriched membrane platforms. Apoptosis 12:1533–1541